3-1-2007

Human Immunodeficiency Virus Type 1 Pathobiology Studied in Humanized BALB/c-Rag2$^{-/-}$ $\gamma_c^{-/-}$ Mice

Santhi Gorantla
University of Nebraska Medical Center

Hannah Seller
University of Nebraska Medical Center

Lisa Walters
University of Nebraska Medical Center

John G. Sharp
University of Nebraska Medical Center

Samuel Pirruccello
University of Nebraska Medical Center

See next page for additional authors

JOURNAL OF VIROLOGY, Mar. 2007, p. 2700–2712 Vol. 81, No. 6
0022-538X/07/$08.00+0 doi:10.1128/JVI.02010-06

Human Immunodeficiency Virus Type 1 Pathobiology Studied in Humanized BALB/c-Rag2$^{-/-}\gamma_c^{-/-}$ Mice$^{\nabla}$

Santhi Gorantla,[1] Hannah Sneller,[1] Lisa Walters,[1] John G. Sharp,[3] Samuel J. Pirruccello,[4] John T. West,[5] Charles Wood,[5] Stephen Dewhurst,[6] Howard E. Gendelman,[1,2] and Larisa Poluektova[1]*

Center for Neurovirology and Neurodegenerative Disorders and Department of Pharmacology and Experimental Neuroscience[1] and Departments of Internal Medicine,[2] Genetics, Cell Biology and Anatomy,[3] and Pathology and Microbiology,[4] University of Nebraska Medical Center, Omaha, Nebraska; Nebraska Center for Virology and School of Biological Sciences, University of Nebraska-Lincoln, Lincoln, Nebraska[5]; and Department of Microbiology and Immunology and James P. Wilmot Cancer Center, University of Rochester Medical Center, Rochester, New York[6]

Received 14 September 2006/Accepted 13 December 2006

The specificity of human immunodeficiency virus type 1 (HIV-1) for human cells precludes virus infection in most mammalian species and limits the utility of small animal models for studies of disease pathogenesis, therapy, and vaccine development. One way to overcome this limitation is by human cell xenotransplantation in immune-deficient mice. However, this has proved inadequate, as engraftment of human immune cells is limited (both functionally and quantitatively) following transplantation of mature human lymphocytes or fetal thymus/liver. To this end, a human immune system was generated from umbilical cord blood-derived CD34$^+$ hematopoietic stem cells in BALB/c-Rag2$^{-/-}\gamma_c^{-/-}$ mice. Intrapartum busulfan administration followed by irradiation of newborn pups resulted in uniform engraftment characterized by human T-cell development in thymus, B-cell maturation in bone marrow, lymph node development, immunoglobulin M (IgM)/IgG production, and humoral immune responses following ActHIB vaccination. Infection of reconstituted mice by CCR5-coreceptor utilizing HIV-1$_{ADA}$ and subtype C 1157 viral strains elicited productive viral replication and lymphadenopathy in a dose-dependent fashion. We conclude that humanized BALB/c-Rag2$^{-/-}\gamma_c^{-/-}$ mice represent a unique and valuable resource for HIV-1 pathobiology studies.

A genetically modified immunodeficient mouse with truncation or knockout of the interleukin-2 (IL-2) receptor (common cytokine receptor) gamma chain (γ_c) provides a unique platform for permanent engraftment of human hematopoietic stem cells (HSCs). The attenuation of cell signaling pathways via γ_c for IL-2, -4, -7, -9, -15, and -21 cytokines, which are involved in survival, differentiation, and function of lymphocytes, impairs the development of mouse lymphatic compartments. This provides a niche for human lymphoid and myeloid cell reconstitution and results in the development of a functional human immune system (HIS).

Development of a functional HIS in mice has been reported to occur in a variety of genetic backgrounds, including NOD/SCID/γ_c^{null} (11, 14, 31), BALB/c-Rag2$^{-/-}\gamma_c^{-/-}$(27), H-2^d-Rag2$^{-/-}$ IL-2R$\gamma_c^{-/-}$(7, 15, 24), and NOD/LtSz-*scid* IL-2Rγ_c^{null} (13, 26). For our studies we used newborn BALB/c-Rag2$^{-/-}\gamma_c^{-/-}$ mice, which we engrafted with CD34$^+$ HSCs (these are referred to hereafter as HIS mice). Previous work has described the generation of all major human lymphoid and myeloid cell types in this model, following HSC engraftment, but the utility of the model has been limited due to variability of HIS reconstitution (18, 27). Attempts to reduce the variability of reconstitution in BALB/c-Rag2$^{-/-}\gamma_c^{-/-}$ mice involved high-dose total body irradiation of newborn pups and administration of granulocyte-macrophage colony-stimulating factor (GM-CSF) (18) and myeloablative regimens consisting of busulfan administration to pregnant females followed by irradiation of newborn pups, or busulfan alone (32).

Current humanized mouse models include transplantation of mature peripheral blood lymphocytes (PBL) (hu-PBL mice [21]) or fetal thymus/liver (SCID-hu mice [22]). Both models do not permit the analysis of human immunodeficiency virus type 1 (HIV-1) replication within the context of an intact human immune system (29). We therefore conducted experiments to examine HIV-1 replication in mice that were engrafted with a functionally active HIS.

The CCR5-utilizing subtype B viral strain ADA (6) and the subtype C isolate 1157 (33) were used for infection of HIS mice. Animals were observed for 8 to 10 weeks after infection. Over this time period, HIS mice infected with HIV-1$_{ADA}$ at high dose developed an inversion of the CD4/CD8 T-cell ratio in peripheral blood as well as lymph node infiltration with CD8$^+$ and immunoglobulin G [IgG]-producing cells similar to those observed in HIV-1-infected humans. Only 50% of animals infected with subtype C HIV-1 had detectable viremia and HIV-1 p24-positive cells in lymphoid tissues. There was no detectable change in the CD4/CD8 T-cell ratio in the peripheral blood of these mice. We conclude that HIS mice retain human cell engraftment for more than 7 months. They can be experimentally infected with HIV-1 and, following HIV-1 infection, animals develop changes in engrafted human lymphoid tissues, which resemble those found in HIV-1-positive human subjects. Collectively, these data establish the HIS mouse as a more authentic model system for studies of HIV-1 pathogenesis than previously available mouse models (21, 22). This system affords significant advantages in investigating HIV-1

* Corresponding author. Mailing address: 985880 Nebraska Medical Center, Omaha, NE 68198-5880. Phone: (402) 559-8926. Fax: (402) 559-3744. E-mail: lpoluekt@unmc.edu.

$^{\nabla}$ Published ahead of print on 20 December 2006.

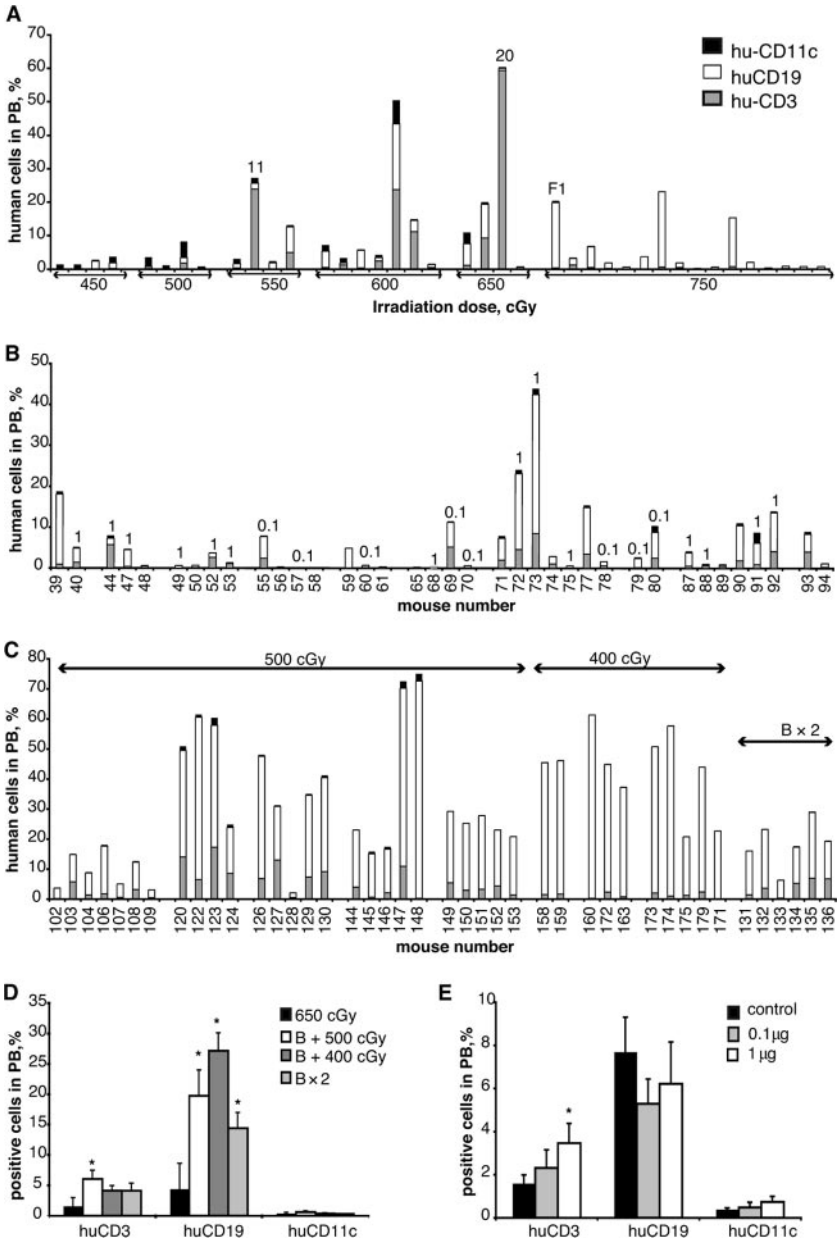

FIG. 1. Human cell reconstitution in mice myeloablated by different protocols and treated with GM-CSF. (A) Determination of optimal doses of irradiation. A significant level of engraftment was achieved at an irradiation dose of between 500 and 650 cGy. A dose of 400 cGy was not effective (not shown). (B) Effect of GM-CSF administration. Newborn pups were irradiated at 650 cGy and injected subcutaneously with GM-CSF every day for 3 weeks (0.1 or 1 μg/dose/mouse) starting at 1 or 2 weeks of age. The number of human cells in the circulation was analyzed 4 weeks after last injection. (C) Effects of intrapartum busulfan administration. Pregnant dams were injected subcutaneously with 15 mg/kg of busulfan solution once, at day 18 postcoitus, and pups were irradiated after birth with 500 cGy or 400 cGy. In the last group busulfan was injected at days 15 and 18 and pups were not irradiated (B × 2). The animals were segregated by litter; each litter received the same $CD34^+$ cell sample. Individual mouse profiles are presented in panels A, B, and C. Numbers above bars correspond to the mouse number (A) and doses of GM-CSF (B). (D) Statistical analysis of the efficacy of different myeloablative procedures presented in panels B and C. The groups were compared to irradiated mice alone. Results are expressed as means ± SEMs. (E) Statistical analysis of the effects of GM-CSF in irradiated animals. *, $P < 0.05$ by ANOVA.

pathobiology as well as exploring new therapeutic and vaccine strategies.

MATERIALS AND METHODS

Mice. $Rag2^{-/-}\gamma_c^{-/-}$ mice were obtained from the Central Institute of Experimental Animals (Kawasaki, Japan) and were bred and maintained under specific-pathogen-free conditions in accordance with ethical guidelines for care of laboratory animals at the University of Nebraska Medical Center as set forth by the National Institutes of Health.

$CD34^+$ cell isolation. Human cord blood was obtained, with parental written informed consent, from healthy full-term newborns (Department of Gynecology and Obstetrics, University of Nebraska Medical Center). After density gradient centrifugation, $CD34^+$ cells were enriched using immunomagnetic beads according to the manufacturer's instructions ($CD34^+$ selection kit; Miltenyi Biotec Inc., Auburn, CA). Numbers and purity of $CD34^+$ cells were evaluated by fluores-

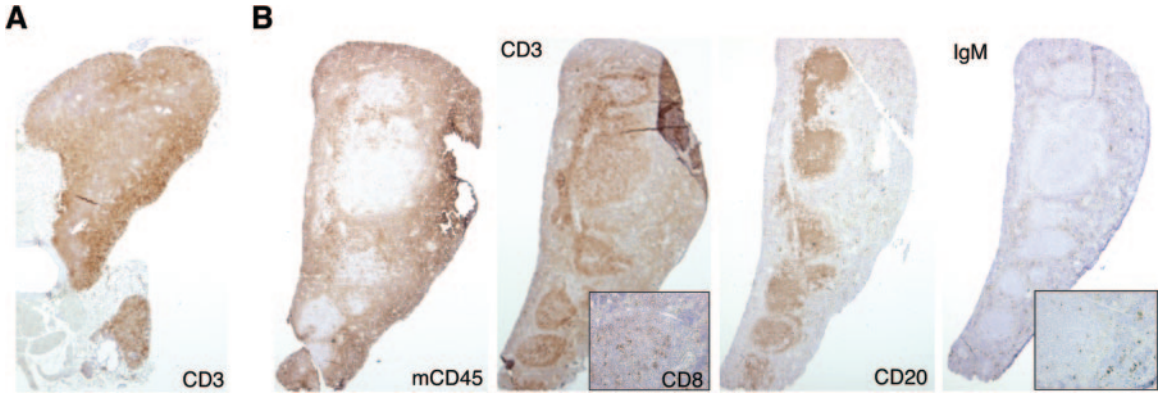

FIG. 2. Thymus and spleen morphology of reconstituted mice. Light microscopic images of paraffin-embedded thymus (23-week-old mouse) and spleen (21-week-old mouse) sections are shown. (A) The thymus tissue contains well-defined cortical and medullary areas. (B) Splenic sections were stained for human CD3, CD20, CD8, and CD68 and mouse CD45 cell markers (diaminobenzidine [DAB]). Sections were counterstained with hematoxylin. Magnification, ×20. Mouse $CD45^+$ cells surround follicles occupied by human $CD3^+$ T cells and a smaller number of $CD8^+$ cells (inset; magnification, ×200), $CD20^+$ B cells and small numbers of IgM-producing plasma cells (inset; magnification, ×200) were distributed in the marginal zone and red pulp.

cence-activated cell sorting (FACS). $CD34^+$ cell purity was >90%. Cells were either frozen or immediately transplanted into newborn mice at 10^4/mouse intrahepatically. From two to seven littermates were reconstituted with one cord blood sample derived from one donor. The numbers of animals reconstituted were dependent on the number of $CD34^+$ cells isolated from cord blood.

Irradiation and busulfan administration. On the day of birth, newborn mice were irradiated twice using a C9 cobalt 60 source (Picker Corporation, Cleveland, OH) at a 3- to 4-h interval. Titrated sublethal doses of 650 cGy, then reduced to 500 and 400 cGy, were used after administration of busulfan to pregnant dams. Busulfan was dissolved in dimethyl sulfoxide (both from Sigma Chemical Co., St. Louis, MO) and administered at a concentration of 15 mg/kg as a 20% dimethyl sulfoxide solution subcutaneously to pregnant dams at day 18 postcoitus. At 4 to 12 h postirradiation, mice were transplanted with $CD34^+$ cells in 20 μl phosphate-buffered saline intrahepatically using a 30-gauge needle. Newborns always received cells from single donors. Mice were weaned at 3 weeks of age.

Virus stocks. The CCR5 coreceptor-utilizing HIV-1_{ADA} strain was propagated in monocyte-derived macrophages cultured for 7 days in the presence of macrophage colony-stimulating factor (a generous gift from Wyeth, Inc., Cambridge, MA) (6). Subtype C HIV-1_{C1157} (CCR5) (33), NL4-3 (CXCR4), and UG 029A (CCR5) viral strains were propagated in phytohemagglutinin (PHA)-stimulated peripheral blood mononuclear cells in the presence of interleukin-2 (BD Bioscience, San Jose, CA) (PHA/IL-2 lymphoblasts). Viral preparations were screened and found to be negative for endotoxin (<10 pg/ml) (Associates of Cape Cod, Woods Hole, MA) and mycoplasma (Gen-Probe II; Gen-Probe, San Diego, CA). The viral titers were assayed on PHA/IL-2 lymphoblasts and monocyte-derived macrophages. Titers were 10^6 and 10^5 50% tissue culture infectious doses ($TCID_{50}$)/ml for HIV-1_{C1157} and HIV-1_{ADA}, respectively.

HIV-1 infection in hu-PBL-BALB/c-Rag2$^{-/-}\gamma_c^{-/-}$ and HIS (BALB/c-Rag2$^{-/-}\gamma_c^{-/-}$) mice. BALB/c-Rag2$^{-/-}\gamma_c^{-/-}$ mice were injected with 30×10^6 human PBL obtained from HIV-1, HIV-2-, and hepatitis B virus-seronegative donors as described previously (6, 23). One week after reconstitution, HIV-1 strains ADA, NL4-3, and UG 029A (subtype B) and C1157 (subtype C) were injected intraperitoneally (i.p.) at 10^2 and 10^4 $TCID_{50}$. Two weeks after infection, the levels of HIV-1 p24 protein in serum and the numbers of $CD4^+$ and $CD8^+$ cells in spleens were analyzed.

HIS (BALB/c-Rag2$^{-/-}\gamma_c^{-/-}$) mice at 16 to 20 weeks were infected i.p. with HIV-1_{1157} ($n = 14$) and HIV-1_{ADA} ($n = 3$) at 10^2 and 5×10^2 $TCID_{50}$, respectively. Since only a single mouse showed detectable levels of HIV-1 p24 in plasma at 2 weeks following this initial exposure to virus, the animals were reinfected with 10^3 and 3.5×10^4 $TCID_{50}$, respectively.

Flow cytometry. Peripheral blood samples were collected from the submandibular vein by using lancets (MEDIpoint, Inc., Mineola, NY) in EDTA-coated tubes. Blood leukocytes and suspensions of spleen cells were tested for mouse CD45 and human pan-CD45, CD45RO, CD45RA, CD3, CD4, CD8, CD11c, CD14, CD19, CD25, CD56, CD123, and HLA-DR markers as four-color combinations (fluorescein isothiocyanate conjugated, phycoerythrin [PE]-cyanin 5.1 conjugated, PE conjugated, and allophycocyanin conjugated). Antibodies as well as isotype controls were obtained from BD PharMingen, San Diego, CA, and staining was analyzed with a FACSCalibur using CellQuest software (BD Immunocytometry Systems, Mountain View, CA). Results were expressed as percentages of total numbers of gated lymphocytes.

Isolated bone marrow cells and thymocytes were stained with fluorescein isothiocyanate-conjugated antibodies (CD8, CD10, and CD33), PE-conjugated antibodies (CD4, CD11c, CD19, and CD235a), PE-Texas red (ECD)-conjugated antibodies (CD3, CD4, CD24, and CD34), PC5-conjugated antibodies (CD2, CD8, CD34, and CD117), and PE-cyanin 7-conjugated antibodies (CD3 and CD45). T-cell receptor (TCR) beta chain expression profiles were analyzed with the IOTest Beta Mark TCR V beta repertoire kit from Beckman Coulter according to the manufacturer's specifications. Data were collected on a Beckman Coulter FC500 flow cytometer (Beckman Coulter, Miami, FL) using Beckman Coulter Cytomics CXP software (Applied Cytometry Systems, Dinnington, United Kingdom). Results were expressed as percentages of total human $CD45^+$ cells.

Immunohistochemistry. Tissue samples (spleen, lymph node, thymus, liver, lung, gut, kidney, and brain) were fixed with 4% paraformaldehyde overnight and embedded in paraffin. Five-micrometer-thick sections were stained with mouse monoclonal antibodies for vimentin (clone 3B4, 1:50), CD68 (clone KP-1, 1:50), HLA-DR (clone CR3/43, 1:100), CD8 (clone 144, 1:50), CD20 (clone L26, 1:50), HIV-1 p24 (clone Kal-1, 1:10), and CD3 (1:100, rabbit polyclonal), all from Dako (Carpinteria, CA). Biotinylated anti-IgG, -IgM, and -IgA antibodies were used at a 1:200 dilution (Vector Laboratories, Burlingame, CA).

Immunoglobulin and HIV-1 p24 measurements. The plasma levels of IgG, IgM, and IgA were determined by enzyme-linked immunosorbent assay (ELISA) (Bethyl, Montgomery, TX). The levels of HIV-1 p24 in the plasma were determined by ELISA (Beckman Coulter, Inc., Brea, CA) according to the manufacturer's instructions.

ELISA and Western blot tests. Plasma samples collected from infected animals were analyzed for HIV-1-specific human antibodies by Genetic Systems HIV-1/HIV-2 enzyme immunoassay (Bio-Rad Laboratories, Hercules, CA) and by Western blotting with HIV-1 nitrocellulose strips (Calypte, Alameda, CA). The strips were incubated overnight in 1:5 diluted serum samples with shaking at 4°C, and horseradish peroxidase-conjugated anti-human IgM and IgG was used as a secondary antibody. The strips were developed using a chemiluminescent substrate (Pierce Biotechnology, Inc., Rockford, IL) and were exposed to X-ray film. HIV-1-positive and -negative human sera were used as positive and negative controls, respectively, at a dilution of 1:1,000.

ActHIB vaccination and humoral immune responses. One-fifth (2 μg) of a single human dose of *Haemophilus influenzae* type b (HIB) conjugate vaccine ActHIB (Aventis Pasteur Inc., Swiftwater, PA) was injected into mice i.p. at 24 to 27 weeks of age. A second injection was delivered 2 weeks later. Mice were killed 3 weeks after the last injection, and the levels of HIB-specific IgG were determined by ELISA according to the manufacturer's instructions (The Binding site, Inc., San Diego, CA).

Statistical analysis. Data were analyzed using Excel software; statistical tests employed were the Student's *t* test (for pairwise comparisons) and one-way analysis of variance (ANOVA) for comparisons of multiple groups. A *P* value of

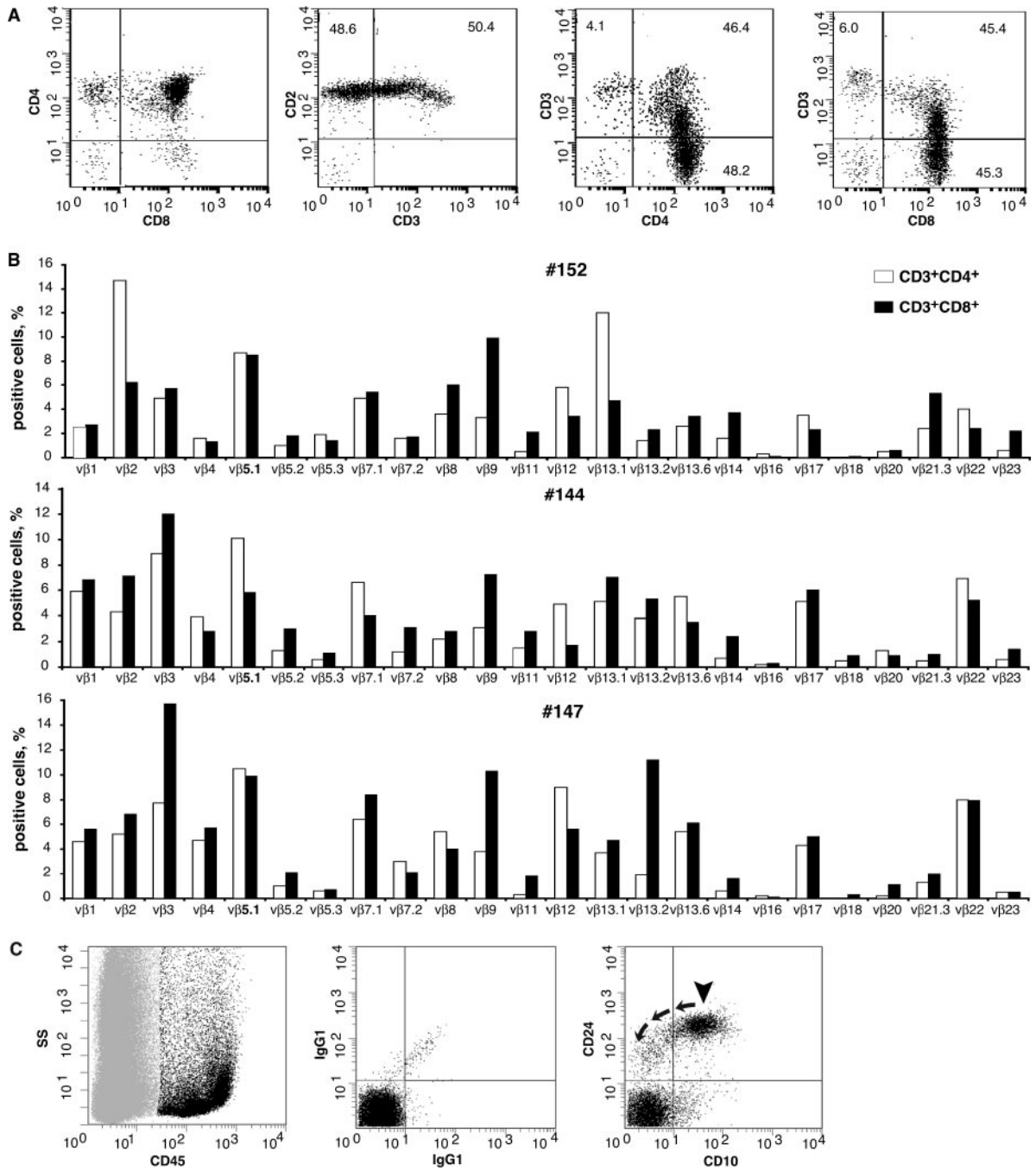

FIG. 3. Thymocyte development, human TCR Vβ repertoire in spleens, and B cells in bone marrow of 18-week-old HIS mice. (A) Dot plots show $CD45^+$ human thymocytes stained for $CD4^+$, $CD8^+$, $CD2^+$, and $CD3^+$ (two left panels). The results demonstrate that the majority of human cells isolated represent CD4 and CD8 dual-positive common thymocytes and that there is also generation of both CD4 and CD8 single-positive, mature T cells. The two plots on the right demonstrate the characteristic increase in thymocyte CD3 density that occurs during thymic maturation/selection. (B) The TCR repertoire of human T cells in the spleen of the same mouse (no. 152) is shown. TCR repertoire profiles for two additional mice from different litters (mice no. 144 and 147) are also shown. (C) B cells in bone marrow of the same mouse no. 152. Plots show CD45-positive human cells (black) and CD45-negative mouse cells (light gray) on a side light scatter (left). The middle plot shows background staining of the human cell population with IgG1 control antibodies for human CD45-positive events. The right plot demonstrates phenotypically normal human B-cell precursors (arrowhead) for human CD45-positive events. These precursors are CD10 and CD24 positive and show differentiation (arrows) to mature B cells as evidenced by a loss of CD10 expression and a decrease in CD24 antigen density.

TABLE 1. Human bone marrow cell subset distributions in engrafted mouse bone marrow[a]

Mouse no.	% of human CD45$^+$ cells positive for:							
	CD34$^+$ (blast)	CD34$^+$ CD117$^+$ (myeloblast)	CD117$^+$ CD33$^+$ (promyelocyte)	CD117$^+$ CD33$^-$ (erythroblast)	CD33$^+$ (myeloid cell)	CD19$^+$ CD34$^+$ (pre-pre-B cell)	CD19$^+$ CD10$^+$ (precursor B cell)	CD19$^+$ (B cell)
152	10.4	6.1	3.1	9.4	8.3	5.6	43.0	48.9
179	11.6	2.8	2.1	4.1	13.9	8.8	34.1	53.0

[a] Percentage of human CD45$^+$ cells positive for the indicated antigen(s) in bone marrow isolated from two representative mice engrafted with CD34$^+$ human hematopoietic stem cells.

<0.05 was considered statistically significant. All results are presented as means ± standard errors of the means (SEMs).

RESULTS

Improvement of reconstitution by myeloablation with busulfan and administration of GM-CSF. Different myeloablation procedures were evaluated in order to optimize human immune cell reconstitution in mice. Irradiation doses ranging from 500 to 750 cGy were sufficient for engraftment of human CD34$^+$ cells in newborn pups (Fig. 1A and B). At 10 to 14 weeks of age, 18 of 75 engrafted mice contained >10% of human cells in their peripheral circulation. The highest doses of irradiation led to significant retardation of animal growth, induction of seizures, and abnormalities of gait secondary to cerebellar aplasia.

Injection of busulfan to pregnant dams (day 18 postcoitus) at 15 mg/kg followed by 500- or 400-cGy irradiation of newborn pups resulted in high levels of human immune cell reconstitution. Here, after 8 to 10 weeks, 36 out of 42 engrafted mice contained >10% of human cells in their peripheral circulation. One-third of these animals had >40% of human cells in their blood (Fig. 1C and D).

In order to increase the numbers of engrafted human immune cells in irradiated mice, GM-CSF was administered for 3 weeks at a dose of either 0.1 or 1 μg/mouse/day, starting at 1 or 2 weeks after reconstitution with CD34$^+$ HSCs (Fig. 1B and E). The number of circulating human cells was analyzed at 4 to 5 weeks after the last GM-CSF administration. The GM-CSF dose of 1 μg/mouse/day resulted in a statistically significant increase in the number of CD3$^+$ T cells in circulation, as well as in the number of myeloid CD11c$^+$ cells; the latter effect did not, however, reach statistical significance.

Representative immunohistology data from the thymuses and spleens of mice reconstituted with human CD34$^+$ HSCs are shown in Fig. 2. There was no discernible difference in tissue morphology between the various groups of animals/myeloablative regimens. The thymus and spleen contained large numbers of human lymphocytes but few human CD68$^+$ cells. Spleens contained follicular structures composed of human T and B cells. CD8$^+$ T cells were limited in numbers, while IgM-producing plasma cells were present only in the "marginal zone" and red pulp (Fig. 2). IgG-producing cells were rare (data not shown).

FACS analysis of representative thymuses and TCR Vβ chain repertoire analysis of human T cells in the spleens of 18-week-old mice (Fig. 3A and B) confirmed the development of polyclonal human T cells de novo. Human B-cell maturation and differentiation in mouse bone marrow were also confirmed by FACS (Fig. 3C; Table 1).

A human immune system was sustained in 7.5-month-old animals. The proportions of human cells phenotyped as CD45$^+$, CD3$^+$, CD19$^+$, CD11c$^+$, and CD123$^+$ in the spleens of nine selected animals (three from each myeloablation protocols) were 18.8% ± 5.3% (range, 7.5% to 31%), 6% ± 1.9%

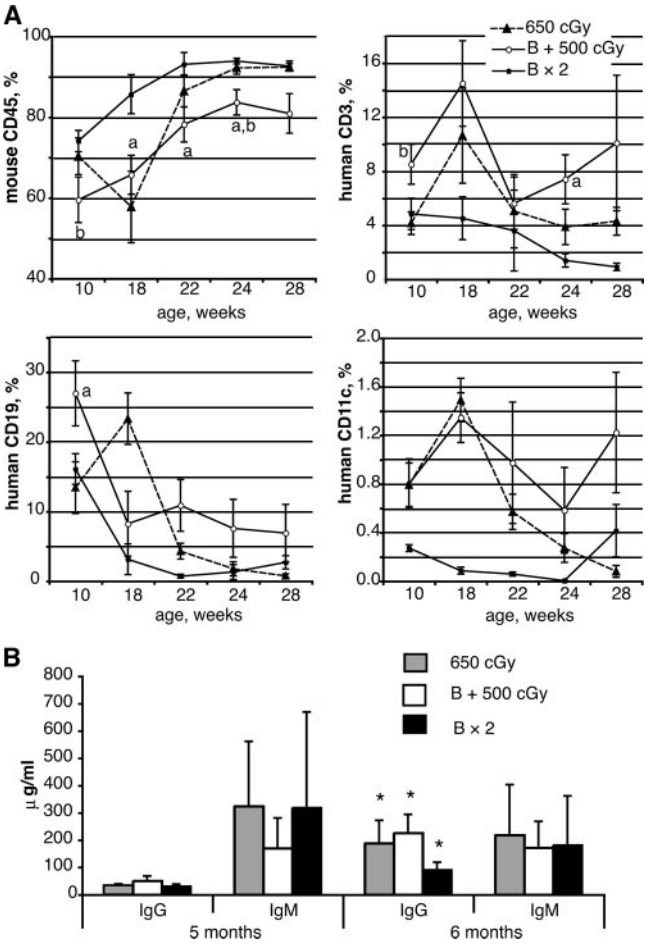

FIG. 4. Profiles of peripheral blood from reconstituted mice. (A) Kinetics of mouse CD45 and human T, B, and CD11c-positive cells in peripheral blood. Error bars indicate SEMs. (B) Human IgG and IgM levels in peripheral blood at 5 and 6 months postreconstitution. The three groups of mice represent animals that were myeloablated using high-dose irradiation alone (650 cGy; $n = 8$), a combination of busulfan plus lower-dose irradiation (B + 500 cGy; $n = 11$), or busulfan alone (B × 2; $n = 5$). In panel A, "a" denotes statistically significant differences between mice irradiated and pretreated with busulfan (B + 500 cGy) and the other two groups, and "b" denotes statistically significant differences between mice myeloablated by the combination of irradiation and busulfan (B + 500 cGy) and animals treated with busulfan alone (B × 2) ($P < 0.05$ by ANOVA). In panel B, * denotes statistically significant differences between IgG levels in 5- and 6-month-old mice.

TABLE 2. Survival rates and efficacy of engraftment

Myeloablation protocol	No. surviving[a]/ total (% surviving)	No. of graft failures[b] (age, wk)
Irradiation (650 cGy)	4/8 (50)	1 (24)
Busulfan (15 mg/kg) + irradiation (500 cGy)	10/11 (90)[c]	3 (30–32)
Busulfan (2 doses of 15 mg/kg)	5/5 (100)	1 (18)

[a] Number surviving >30 weeks.
[b] Loss of the graft is defined as the presence of <1% circulating human cells in blood.
[c] Difference between irradiation alone (650 cGy) and combination of busulfan with a lower dose of irradiation, $P < 0.04$ by chi test.

(0.9% to 14.9%), 4.3% ± 2.3% (0.12% to 17.4%), 0.6% ± 0.3% (0.03% to 2.45%), and 0.9% ± 0.8% (0.1% to 3.6%), respectively. The proportion of human $CD45^+$ cells in bone marrow was 6.6% ± 4.5% (1.79% to 31%), and both myeloid ($CD117^+$ $CD33^+$) and erythroid ($CD117^+$ $CD33^-$) progenitors were detected (Table 1). Furthermore, all tested animals also retained lineage-negative $CD34^+$ HSCs in the bone marrow.

In order to characterize the kinetics of repopulation and maturation of the HIS, the mouse peripheral blood was analyzed. Three groups of animals were evaluated: (i) eight newborn pups that received irradiation alone, (ii) 11 pups whose mothers were treated with busulfan following 500 cGy of irradiation on the day of delivery, and (iii) 5 pups whose mothers received busulfan during pregnancy at days 15 and 18 postcoitus. These animals were observed for survival and for the presence of human cells in blood (Fig. 4A; Table 2). High-dose-irradiated mice showed poor survival compared to mice treated with a combination of busulfan and irradiation. There was no mortality in the group of animals treated only with busulfan (Table 2). These animals remained fertile, delivered pups, and also retained engrafted human cells (data not shown).

The first wave of human cells in mouse blood represented, in significant measure, expansion of $CD19^+$ B cells. Maximal numbers of human T cells in circulation were not observed until 18 to 20 weeks postengraftment (Fig. 4). After 22 weeks, the number of T cells in the peripheral blood stabilized and in some animals even increased. The proportion of $CD19^+$ B cells diminished at 18 weeks of age. Recipients that were only irradiated had a slower expansion of human cells than the animals that received the combination of busulfan pretreatment and reduced-dose irradiation.

Significant IgG production was first observed in 5-month-old mice (Fig. 4B). In two animals high IgM levels (1,231 and 1,580 μg/ml) were detected at 5 months of age, which subsequently declined (to 669 and 1,244 μg/ml), coinciding with the increased IgG production (from 44 to 150 and from 9.5 to 33 μg/ml, respectively) at 6 months. IgA levels were low in all mice tested.

Taken together, these findings show that myeloablation protocol, which included busulfan administration, significantly improved mouse survival, as well as human immune cell reconstitution in BALB/c-Rag2$^{-/-}\gamma_c^{-/-}$mice. GM-CSF administration had minimal effects. Full maturation of the HIS in the engrafted mice, as reflected by the ability to produce IgG, required 5 to 6 months

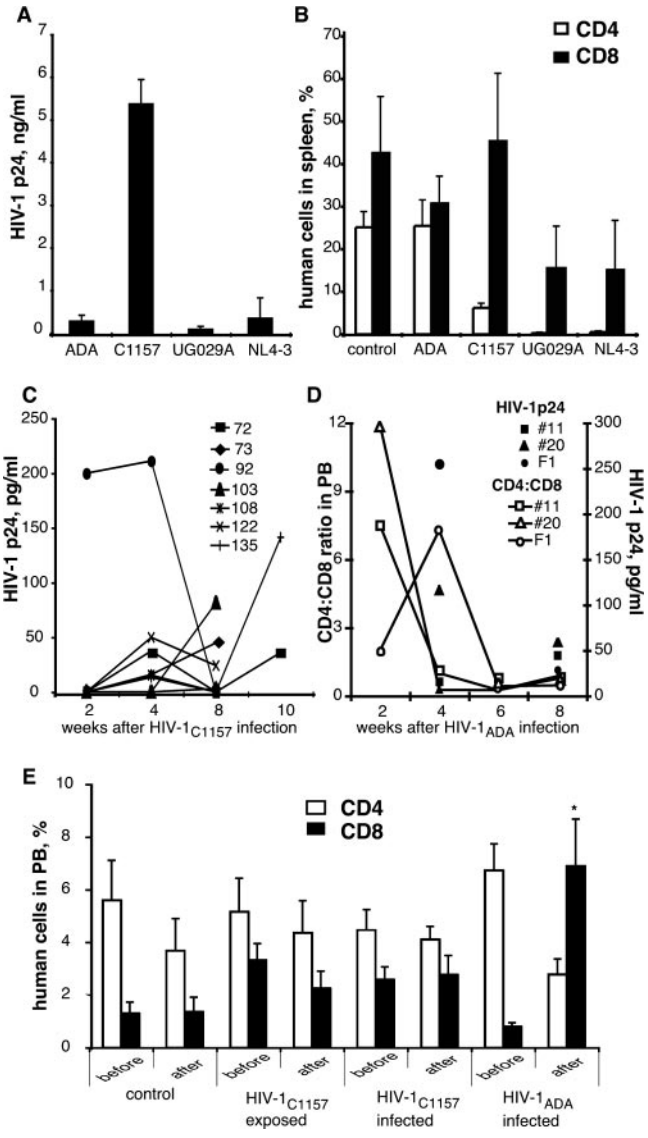

FIG. 5. Viral replication and cytopathic effects of different HIV-1 strains in hu-PBL-Rag2$^{-/-}\gamma_c^{-/-}$ mice and HIS BALB/c-Rag2$^{-/-}\gamma_c^{-/-}$ mice. Adult Rag2$^{-/-}\gamma_c^{-/-}$ mice ($n = 4$ per group) were injected with human PBL (30×10^6 cells/mouse). One week later mice were infected i.p. by the indicated strains of HIV-1 at a dose of 10^2 $TCID_{50}$. Plasma and splenocytes were collected 2 weeks after infection and analyzed for the levels of HIV-1 p24 antigen in circulation (A) and for the presence of human CD4 and CD8 cells (B). All viruses were tested in three different experiments with mice that were reconstituted with PBL derived from three different donors, and similar results were obtained. Error bars indicate SEMs. (C to E) HIS BALB/c-Rag2$^{-/-}\gamma_c^{-/-}$ mice at 18 to 24 weeks of age were infected with HIV-1 via the i.p. route, using either the C1157 (C) or the ADA (D) isolate. Mice were exposed once to a low-dose inoculum and then exposed to a higher-dose inoculum two weeks later. Blood samples were collected starting at 2 weeks after the first exposure to virus and analyzed for the levels of HIV-1 p24 antigen (C and D), as well as for number of human CD4 and CD8 cells (D and E). (D) Only HIV-1_{ADA}-infected mice showed inversion of the CD4/CD8 ratio. Open symbols represent CD4/CD8 ratios in peripheral blood; closed symbols represent HIV-1 p24 concentrations in plasma. (E) Control mice ($n = 5$), mice exposed to C1157 but without evidence of productive infection ($n = 7$), and mice exposed to C1157 with productive infection ($n = 7$) retained statistically indistinguishable numbers of CD4 and CD8 cells in the analyses before infection and at the end point. Only HIV-1_{ADA}-infected mice showed statistically significant changes in the number of circulating CD8 cells. *, $P < 0.05$.

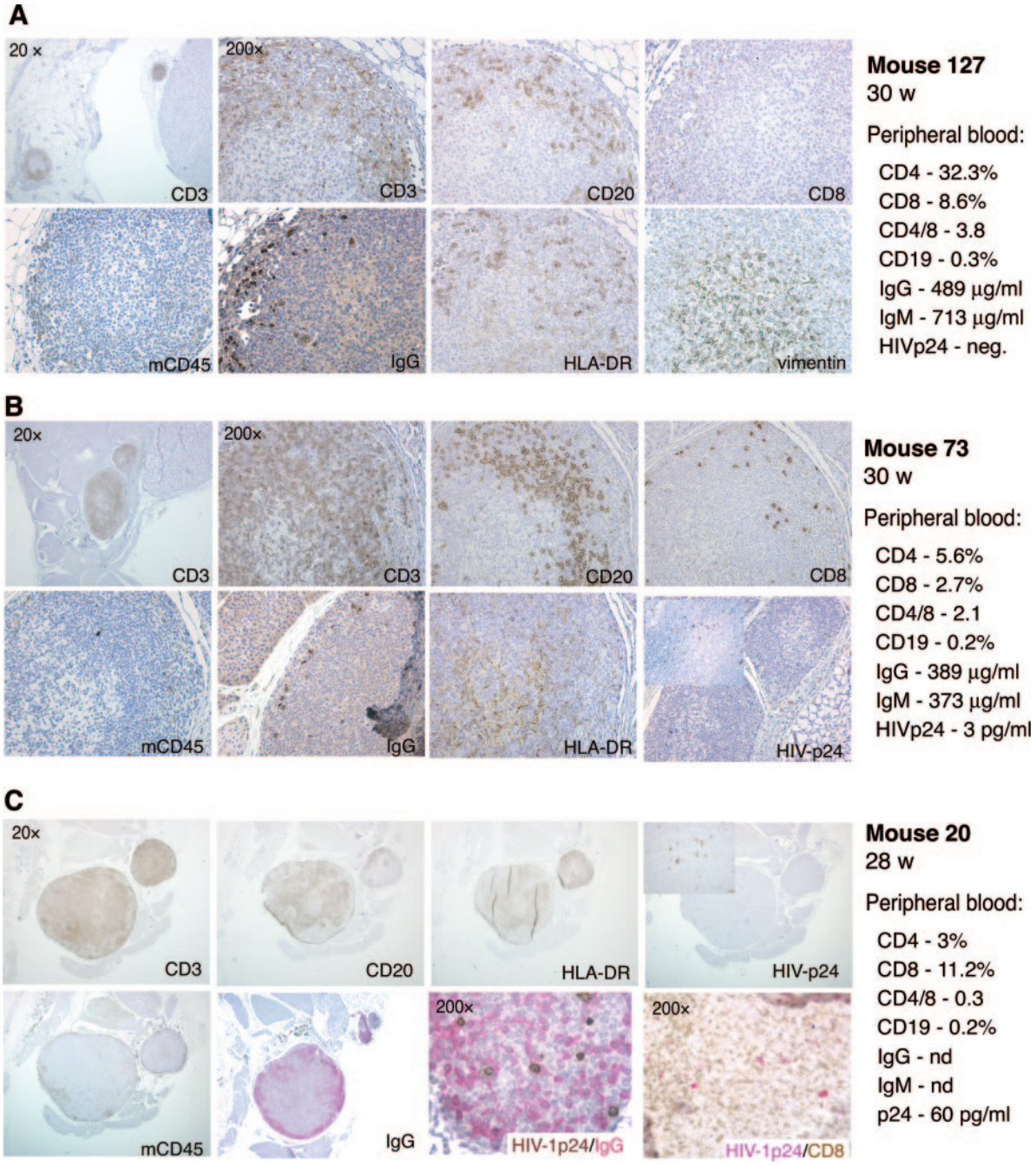

FIG. 6. Pathomorphology of cervical lymph nodes from HIV-1-infected mice. (A) Low- and high-magnification images of two cervical lymph nodes of control mouse 127 are shown. Paraffin-embedded 5-µm sections were stained for human CD3, CD20, CD8, HLA-DR, IgG, and vimentin and mouse CD45 markers. The lymph node contained medullae (characterized by the presence of dendritic cells), a paracortical T-cell region with very few CD8-positive cells, marginal zone B cells, and few IgG-secreting cells. (B) Cervical lymph nodes from HIV-1_{C1157}-exposed mouse no. 73 are shown. No p24 antigen-positive cells were detected in this lymph node, although HIV-1 p24-positive cells were found in spleen from this animal (inset; magnification, ×200). (C) Enlargement of the cervical lymph node from mouse no. 20 infected with HIV-1_{ADA}. This panel also shows infiltration of this lymph node with $CD8^+$ and IgG-producing cells. The right column in each of the panels provides the phenotypic profile of peripheral blood cells from each of the animals, as well as their serum IgG and IgM profiles. Brown, DAB; purple, Permanent Red.

and might be reminiscent of some aspects of pre- and postnatal development of human immunity.

HIV-1 infection of hu-PBL-Rag2$^{-/-}\gamma_c^{-/-}$ mice. HIV-1 infection was first tested in Rag2$^{-/-}\gamma_c^{-/-}$ mice reconstituted with human peripheral blood lymphocytes (hu-PBL-Rag2$^{-/-}\gamma_c^{-/-}$ mice). Animals at 5 weeks of age were injected i.p. with 30×10^6 PBL/mouse. One week after reconstitution, the HIV-1 strains ADA, NL4-3, UG 029A (subtype B), and C1157 (subtype C) were independently injected i.p. at a dose of 10^2 or 10^4 $TCID_{50}$. Two weeks after infection, levels of HIV-1 p24

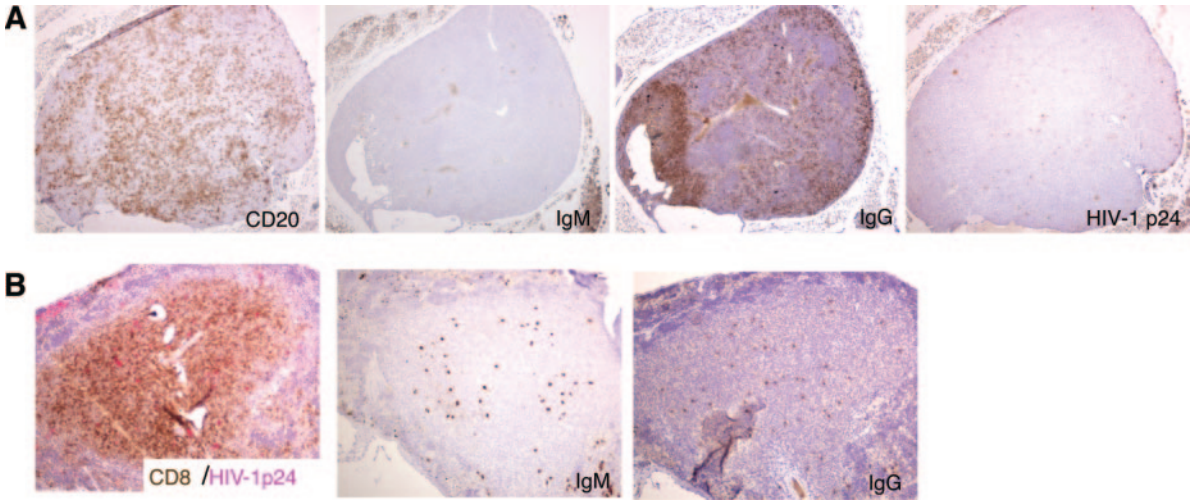

FIG. 7. Representative serial sections of an enlarged mediastenal lymph node and spleen lymphoid follicle from mouse no. 11 infected with HIV-1_{ADA}. (A) Distribution of $CD20^+$ and HIV-1 $p24^+$ cells and infiltration with IgG-producing cells and absence of IgM-producing cells in lymph node. Magnification, ×40. (B) Distribution of $CD8^+$/HIV-1 $p24^+$ cells in a spleen lymphoid follicle; IgM- and IgG-producing cells are also present. $CD8^+$ cells are brown (DAB), and HIV-1 $p24^+$ cells are pink (Permanent Red). Magnification, ×40. The levels of HIV-1 p24 protein in peripheral blood 2 weeks after infection in this animal were undetectable, but after reinfection, HIV-1 p24 antigen was detected in blood at 16 pg/ml (25 weeks) and at 45 pg/ml (29 weeks).

were measured in plasma, and $CD4^+$ and $CD8^+$ cells were enumerated in spleens. As shown in Fig. 5A and B, inoculation of animals with a dose of 10^2 $TCID_{50}$ of HIV-1_{C1157} resulted in a significant viremia with depletion of $CD4^+$ T lymphocytes in spleen. HIV-1_{ADA} also replicated and was detected in the mice, albeit to a lower level than HIV-1_{C1157}. Viral strains NL4-3 and UG 029A elicited a depletion of human $CD4^+$ T lymphocytes. The higher-dose inoculum (10^4 $TCID_{50}$) yielded similar results for all of the strains (data not shown). The subtype C isolate C1157 and HIV-1_{ADA} were selected for infection of HIS mice (Fig. 5C and D).

HIV-1 replication and tissue histopathology in HIS mice. Low doses of viruses (10^2 $TCID_{50}$ for HIV-1_{C1157} [$n = 14$] and 5×10^2 $TCID_{50}$ for HIV-1_{ADA} [$n = 3$]) were injected i.p. in 16- to 20-week-old mice. At 2 weeks after infection, only one mouse inoculated with HIV-1_{C1157} had a detectable level of HIV-1 p24 in the circulation (200 pg/ml). In light of this apparent failure to infect the majority of mice with a low-dose inoculum, the animals were then reinfected at higher doses of viruses (10^3 and 3.5×10^4 $TCID_{50}$ for HIV-1_{C1157} and HIV-1_{ADA}, respectively). Blood samples were collected every 2 to 4 weeks thereafter to quantify HIV-1 p24 and the number of human cells in circulation (CD3, CD19, CD4, and CD8). Eight weeks after exposure to HIV-1_{C1157}, only 7 of 14 infected animals (50%) had detectable levels of HIV-1 p24 in blood, and 6 of them had HIV-1 $p24^+$ cells in their lymphoid tissues (detected at 8 to 10 weeks following virus infection and localized predominantly to the lymph nodes and spleen rather than the thymus). As shown in Fig. 5C, by 8 weeks after viral infection, the level of HIV-1 p24 in the circulation decreased to undetectable levels in some mice. All animals that underwent productive infection by HIV-1_{C1157} (as evidenced by detection of HIV-1 p24 antigen in blood and/or p24 antigen-positive cells in lymphoid tissue) retained $CD4^+$ T lymphocytes in circulation without a significant elevation of $CD8^+$ T lymphocytes. Only animals infected with high viral inoculum of HIV-1_{ADA} showed an increased proportion of $CD8^+$ T lymphocytes in circulation, reduced $CD4^+$ T cells, and an inversion of the CD4/CD8 ratio (Fig. 5D and E). All HIV-1_{ADA}-infected mice had HIV-1 $p24^+$ cells in spleen and lymph nodes.

Cervical lymph node (CLN) histology for control (uninfected) and HIV-1-infected mice, as well as human immune cell profiles in blood, is shown in Fig. 6. All animals developed "miniature" human-like nodes with a central medullar area occupied by dendritic cells, a cortical area with T and B cells, and limited numbers of immunoglobulin-secreting plasma cells. A few $CD8^+$ T lymphocytes were also present in CLN tissues from uninfected mice. In mice infected with HIV-1_{C1157}, an enlargement of CLN tissue was detectable, accompanied by infiltration with $CD3^+$ cells of the medullar region and the presence of HIV-1 p24-positive cells in spleen (but not in lymph nodes) (Fig. 6B). Significant hyperplasia, infiltration with CD8 cells, IgG-producing cells, and abnormal structures were also observed in CLNs from two HIV-1_{ADA}-infected mice (mice 11 and 20) (Fig. 6C and 7). A younger mouse (F1) infected at 16 week of age with single high dose of HIV-1_{ADA} and killed 5 weeks later exhibited significant infiltration of lymph nodes by $CD8^+$ cells and the presence of human $CD68^+$ cells in the mesenteric lymph node capsule (Fig. 8). None of the infected mice were found to produce detectable levels of HIV-1-specific antibodies, as assessed by the Genetic Systems HIV-1/HIV-2 enzyme immunoassay or by Western blot assays (data not shown).

Humoral immune response to ActHIB in HIS mice. To confirm the competence of the humoral immune system in the HIS mice, three mice (24 to 27 weeks of age) were vaccinated with two doses of ActHIB (2 μg/mouse) delivered i.p. with a 2-week interval in between. Plasma samples were collected 3 weeks after the second dose. The humoral immune responses were analyzed by ELISA. All immunized animals developed HIB-

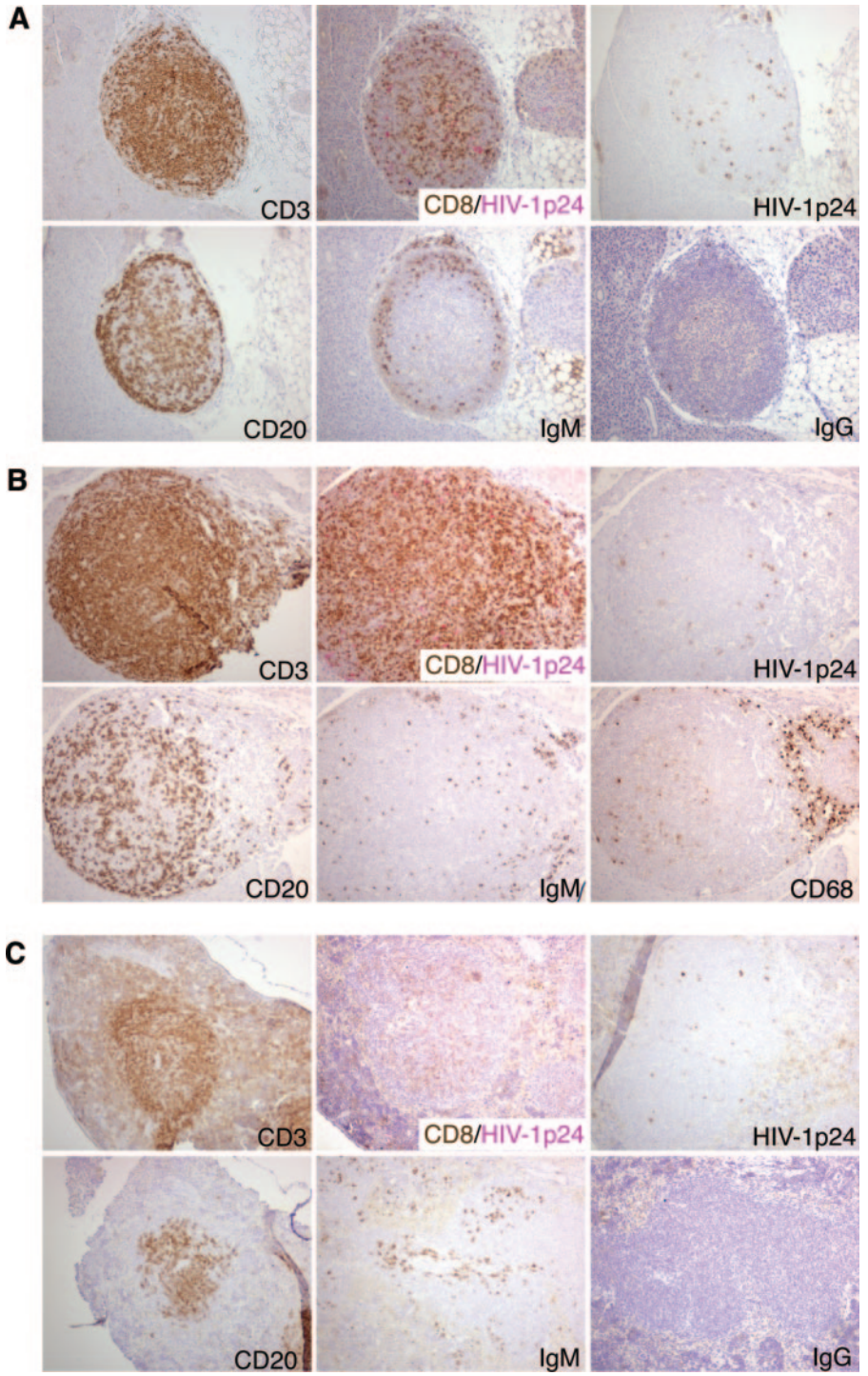

FIG. 8. Immunopathology of lymphoid tissues in HIV-1_{ADA}-infected HIS mouse no. F1. Representative serial sections of cervical (A) and mesenteric (B) lymph nodes and spleen (C) of a mouse infected at 16 weeks of age with HIV-1_{ADA} are shown. The distributions of $CD3^+$, $CD20^+$, $CD68^+$, and HIV-1 $p24^+$ cells are shown, together with infiltration by $CD8^+$ cells. IgM-producing cells were present; however, IgG-producing cells were rare. In double-stained panels $CD8^+$ cells are brown (DAB) and HIV-1 $p24^+$ cells are pink (Permanent Red). Magnification, ×100. The level of HIV-1 p24 protein in peripheral blood 2 weeks after infection was 225 pg/ml, and it dropped to 29 pg/ml by the fifth week after infection.

specific IgG (25), and only one of four nonvaccinated mice had detectable Hib-specific IgG levels (Table 3). FACS analyses of blood, spleen, and bone marrow and morphological analysis of the thymus and spleen from one of these vaccinated mice (mouse 120) are presented in Fig. 9. The thymus of this animal was populated with human T cells, macrophages, and a small number of $CD20^+$ cells (not shown). The spleen was populated with human T, B, myeloid, and plasmacytoid antigen-present-

TABLE 3. Anti-ActHIB responses

Mouse no.	Age (wk) at start of vaccination	% of human cells in blood			IgG (μg/ml)	
		CD3+	CD19+	CD11c+	Total	HIB specific[a]
Vaccinated						
103[b]	27	2.3	1.3	0.06	283.1	1.35
120[c]	25	12.8	2.3	2.3	286.1	2.14
123	25	3.2	1.8	1.3	152.7	0.47
Nonvaccinated, 80[d]	29	2.5	6.4	1.5	155.9	0.14

[a] All vaccinated animals mounted an antigen-specific IgG response consistent with protective humoral immunity.
[b] Vaccinated after HIV-1_{C1157} infection (HIV-1 p24, 81.3 pg/ml at end point).
[c] Exposed to C1157 but did not develop detectable evidence of productive virus infection (no HIV-1 p24 could be detected in blood and tissues).
[d] Three more nonvaccinated mice (no. 127, 131, and 132) were used as controls, and they did not show detectable HIB-specific antibodies.

ing cells. A higher expression of HLA-DR was also detected, and the engrafted human T and B cells were found to be clustered in areas that were reminiscent of germinal-like centers. These findings confirm that HIS mice retain a functional immune system and are able mount humoral immune responses at ages of over 24 weeks.

DISCUSSION

Mice engrafted with human immune cells (mature peripheral blood lymphocytes or fetal thymus/liver transplant under kidney capsule) have emerged as a powerful model for studying the pathogeneses of species-specific virus pathogens, including HIV-1, human T-lymphotropic virus type 1, and human herpesviruses such as varicella-zoster virus and human herpesvirus 6 (8, 12, 20). The ability to engraft human HSCs in small animals is extremely valuable, since it offers a new model system for studies on the ontogeny of the human immune system and for the analysis of the interplay of species-specific pathogens. Recent progress in the generation of humanized mice with long-term reconstitution of human functional lymphoid tissues by transplantation of HSCs was reviewed by Macchiarini et al. (17) and Legrand et al. (16). The best results so far, in terms of the longevity of engraftment and the functional properties of a HIS in a murine environment, have been achieved in mice with a deletion or truncation of IL-2Rγ_c: BALB/c-Rag2$^{-/-}\gamma_c^{-/-}$, NOD/SCID/γ_c^{null}, and NOD/LtSz-*scid* IL-2rγ_c^{null} mice. Such animals can be engrafted with HSCs derived from a range of different sources, including umbilical cord blood, mobilized HSCs from peripheral blood, and fetal liver. However, to date, none of the published protocols has resulted in reproducible, efficient, and uniform engraftment of human immune cells in these mice. The first part of the present work was therefore dedicated to the development of an improved method for the reconstitution of mice with HSCs.

We used BALB/c-Rag2$^{-/-}\gamma_c^{-/-}$ newborn pups in our reconstitution experiments (27) but were unsuccessful in creating stable chimerism using the published irradiation dose of 375 cGy. The irradiation needed to create a niche for the engraftment of human cells was between 550 and 700 cGy. Even a high dose of 650 cGy did not guarantee higher levels of engraftment. Moreover, such doses induced significant health problems and reduced the survival of animals. We therefore combined lower-dose irradiation with busulfan-mediated myeloablation. We based our busulfan regimen on a protocol that was previously used for successful allotransplantation of bone marrow in C57BL/6 mice (7).

Busulfan, a common component of pretransplant conditioning regimens in human bone marrow transplantation (9), selectively destroys quiescent stem cells (2, 4, 10). When combined with a lower (400-cGy) dose of irradiation, the intrapartum busulfan injection yielded efficient, stable, and reproducible engraftment of HSCs. The reduced irradiation dose in this combination regimen resulted in improved outcomes in terms of survival and neurologic damage (seizures or balance abnormalities).

In order to assess the kinetics of maturation of HIS in BALB/c-Rag2$^{-/-}\gamma_c^{-/-}$ mice, we monitored human cells and immunoglobulin levels in peripheral blood. During the early postengraftment period, a significant expansion of CD19+ cells was observed, as previously noted in NOD/SCID/γ_c^{null} mice (11, 13). This may be related, in part, to the presence of immature B-cell precursors in cord blood and to ongoing stimulation of these cells by the murine environment. However, we observed that the expansion of these cells gradually tapered off, and the number of human B cells in circulation began to decline by 22 to 28 weeks after engraftment. At a slightly earlier time point (16 to 20 weeks), the frequency of human T cells in peripheral blood reached a stable peak, and lymph nodes and spleen were populated. Thus, all components of an HIS were present by 16 weeks of age. However, full functional maturation of the HIS was not complete until 5 to 6 months of age, as reflected by the ability to stably produce IgG and to mount a humoral immune response to ActHIB vaccination.

The second aspect of this study focused on an evaluation of HIV-1 infection in HIS mice. Researchers interested in the development of a mouse model for HIV-1 infection previously have used either (i) immune-deficient mice reconstituted with human peripheral blood lymphocytes (hu-PBL mice) (21) or (ii) immune-deficient mice engrafted with fetal human thymus/liver under the kidney capsule (Thy/Liv SCID-hu mice) (1, 19, 22). There was considerable initial enthusiasm for the use of these models to study HIV-1 pathobiology. However, important technical limitations have precluded their widespread use and broad applicability. These limitations include reduced survival of the engrafted human immune cells, graft-versus-host reactions, an incomplete human T-cell receptor repertoire, deficiency of human antigen-presenting cells, and incomplete peripheral lymphocyte reconstitution. Perhaps most importantly, the functional properties of a human immune system were compromised, and HIV-1 infection led to very rapid depletion of human CD4+ T lymphocytes without most of the other hallmarks of HIV-1 infection in human subjects.

We show here that engrafted human immune cells in BALB/c-Rag2$^{-/-}\gamma_c^{-/-}$ mice are susceptible to HIV-1 infection but that the dynamics of virus infection are substantially different in this model than in previously described models such as hu-PBL mice. The HIS mice are less susceptible to low-dose infection with HIV-1 and undergo a slower, more protracted course of CD4+ T-cell depletion compared to hu-PBL mice. This may be because HIS mice contain a larger fraction of naive human T cells than hu-PBL mice. Impor-

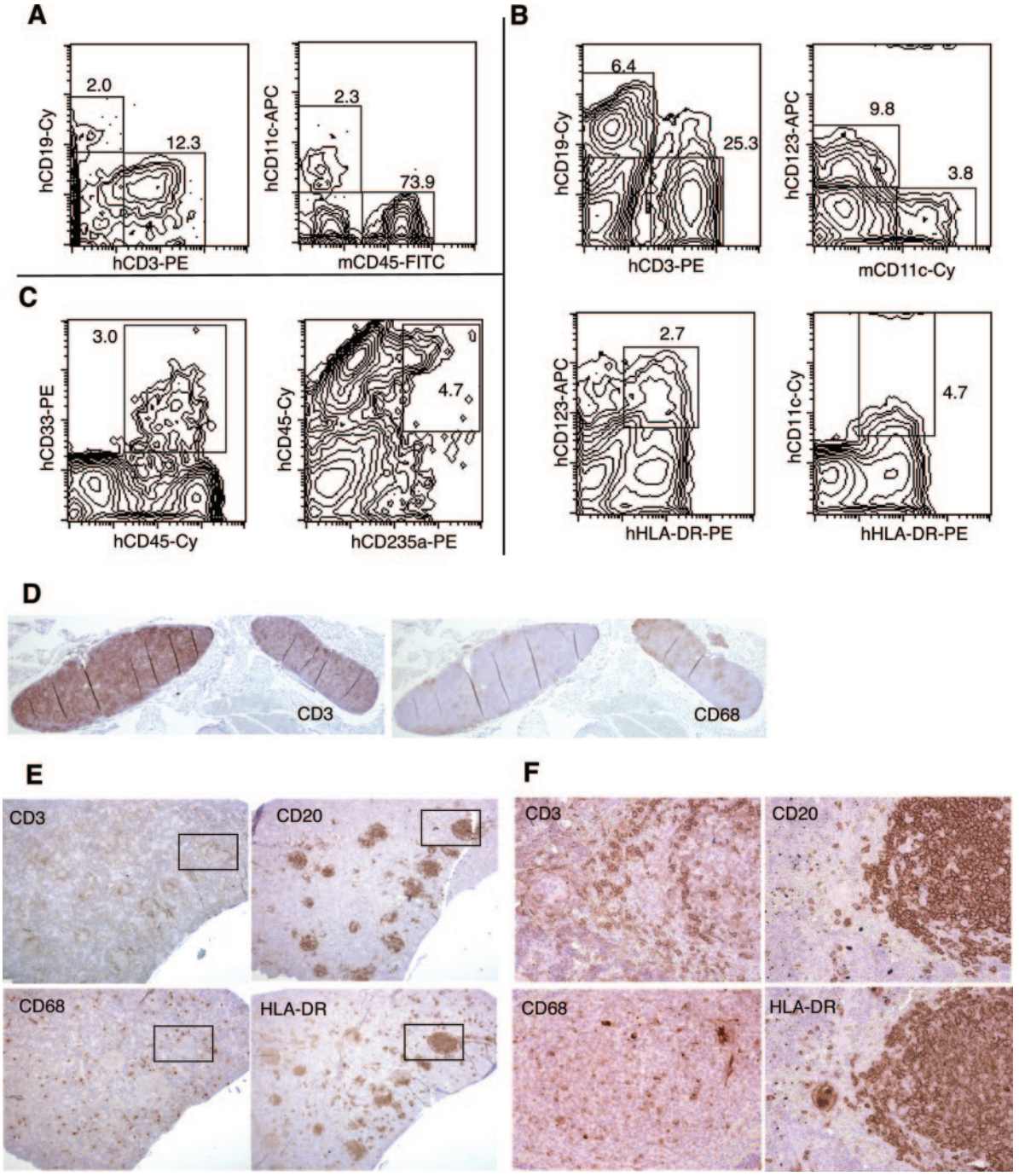

FIG. 9. FACS profiles and/or morphology of peripheral blood, spleen, bone marrow, and thymus from 30-week-old mouse no. 120, which was HIV-1_{C1157} infected and then vaccinated with ActHIB. (A to C) FACS profiles for peripheral blood (A), spleen (B), and bone marrow (C); antibodies were specific for the indicated human (h) or mouse (m) cell surface proteins. (D) Paraffin-embedded sections of two thymus lobes stained for T cells and CD68-positive cells. Magnification, ×20. (E) Spleen sections stained for CD3, CD20, CD68, and HLA-DR markers. Magnification, ×20. (F) Magnified views of selected regions of the same areas in panel A. Magnification, ×200.

tantly, the large number of naive T cells in HIS mice is consistent with what is known about the T-cell population in normal human subjects, and this highlights the biological relevance of this new model.

In HIS mice the cytotoxicity of tested viral isolates did not correspond to the virus behavior in hu-PBL mice, where a rapid depletion of $CD4^+$ cells occurs after administration of HIV-1_{C1157}, as well as NL4-3 and UG 029A. In contrast, the same low doses of HIV-1 did not induce rapid viremia and depletion of $CD4^+$ cells in HIS mice. Indeed, we were able to demonstrate the stable infection of HIS mice with HIV-1_{C1157}, for at least 8 to 10 weeks following virus inoculation. This may

provide a model for analysis of the early stages of natural HIV-1 infection in humans.

Infection of HIS mice with a high dose of HIV-1_{ADA} induced significant activation of the engrafted human immune system, with expansion of $CD8^+$ cells, activation of B cells, and pathomorphologic changes in lymph nodes. These changes were similar to those observed in advanced HIV-1 infection in human subjects and again serve to underscore the relevance of the HIS mouse model for HIV-1 infection. At the same time, it is important to note that we were not able to detect humoral responses against HIV-1 in the HIS mice. This was unexpected, since the animals were capable of mounting an effective humoral immune response against a different antigen. It is possible that reconstitution of mice with HSCs may fail to provide key cells required for the efficient generation of HIV-1-specific humoral immune responses (such as human follicular dendritic cells) (27). It is also possible that induction of humoral immune responses to HIV-1 in HIS mice may require a higher level of virus replication (30) or that virus replication in HIS mice may interfere with B-cell maturation and preclude the generation of a HIV-1-specific antibody response, or it may simply be the case that seroconversion and development of HIV-1-specific humoral immune responses may require more than 10 weeks (3, 5, 28). Further studies will be needed to distinguish these possibilities.

While our studies were in progress, Watanabe and colleagues reported on the outcome of HIV-1 infection in human HSC-transplanted NOD/SCID-IL-2Rγ^{null} mice, following exposure to both low and high doses of HIV-1_{JRCSF}, HIV-1_{MNp}, or SHIV-C/1 (30). These studies showed that virus replication persisted for up to 40 days after inoculation and that it resulted in inversion of CD4/CD8 T-cell ratios in the spleen, at least in some cases. The present work corroborates these findings but also extends them considerably by (i) developing an improved and more reproducible engraftment procedure, (ii) demonstrating stable HIV-1 infection of HIS mice for up to 10 weeks following virus inoculation, and (iii) showing changes in lymphoid architecture that resemble those found in HIV-1-infected humans. These findings establish unequivocally the utility of the HIS model. Overall, we conclude that HIS mice (BALB/c-Rag2$^{-/-}\gamma_c^{-/-}$ mice engrafted with $CD34^+$ human hematopoietic stem cells) are a unique and valuable resource to study early stages of HIV-1 infection in its human host.

ACKNOWLEDGMENTS

This work was supported by grants from the National Institutes of Health (P20RR15635 to L.P., C.W., and H.E.G. and 2R37 NS36126, P01 NS31492, P01 NS43985, and NS034239 to H.E.G.).

We thank Mamoru Ito (Laboratory of Immunology, Central Institute for Experimental Animals, Kawasaki, Japan) for providing the BALB/c-Rag2$^{-/-}\gamma_c^{-/-}$ mice used in this study and information regarding the animals' genetic backgrounds. We thank Linda Wilkie and Victoria Smith for support with FACS and Dawn Eggert for assistance in the breeding of the animals.

REFERENCES

1. **Aldrovandi, G. M., G. Feuer, L. Gao, B. Jamieson, M. Kristeva, I. S. Chen, and J. A. Zack.** 1993. The SCID-hu mouse as a model for HIV-1 infection. Nature **363:**732–736.
2. **Anderson, R. W., K. I. Matthews, D. A. Crouse, and J. G. Sharp.** 1982. In vitro evaluation of hematopoiesis in mice treated with busulphan or nitrogen mustard. Biomed. Pharmacother. **36:**149–152.
3. **Binley, J. M., P. J. Klasse, Y. Cao, I. Jones, M. Markowitz, D. D. Ho, and J. P. Moore.** 1997. Differential regulation of the antibody responses to Gag and Env proteins of human immunodeficiency virus type 1. J. Virol. **71:**2799–2809.
4. **Botnick, L. E., E. C. Hannon, and S. Hellman.** 1979. Nature of the hemopoietic stem cell compartment and its proliferative potential. Blood Cells **5:**195–210.
5. **Cole, K. S., M. Murphey-Corb, O. Narayan, S. V. Joag, G. M. Shaw, and R. C. Montelaro.** 1998. Common themes of antibody maturation to simian immunodeficiency virus, simian-human immunodeficiency virus, and human immunodeficiency virus type 1 infections. J. Virol. **72:**7852–7859.
6. **Gendelman, H. E., J. M. Orenstein, M. A. Martin, C. Ferrua, R. Mitra, T. Phipps, L. A. Wahl, H. C. Lane, A. S. Fauci, and D. S. Burke.** 1988. Efficient isolation and propagation of human immunodeficiency virus on recombinant colony-stimulating factor 1-treated monocytes. J Exp. Med. **167:**1428–1441.
7. **Gimeno, R., K. Weijer, A. Voordouw, C. H. Uittenbogaart, N. Legrand, N. L. Alves, E. Wijnands, B. Blom, and H. Spits.** 2004. Monitoring the effect of gene silencing by RNA interference in human $CD34^+$ cells injected into newborn RAG2$^{-/-}\gamma_c^{-/-}$ mice: functional inactivation of p53 in developing T cells. Blood **104:**3886–3893.
8. **Gobbi, A., C. A. Stoddart, M. S. Malnati, G. Locatelli, F. Santoro, N. W. Abbey, C. Bare, V. Linquist-Stepps, M. B. Moreno, B. G. Herndier, P. Lusso, and J. M. McCune.** 1999. Human herpesvirus 6 (HHV-6) causes severe thymocyte depletion in SCID-hu Thy/Liv mice. J Exp. Med. **189:**1953–1960.
9. **Gupta, V., H. M. Lazarus, and A. Keating.** 2003. Myeloablative conditioning regimens for AML allografts: 30 years later. Bone Marrow Transplant. **32:**969–978.
10. **Hellman, S., L. E. Botnick, E. C. Hannon, and R. M. Vigneulle.** 1978. Proliferative capacity of murine hematopoietic stem cells. Proc. Natl. Acad. Sci. USA **75:**490–494.
11. **Hiramatsu, H., R. Nishikomori, T. Heike, M. Ito, K. Kobayashi, K. Katamura, and T. Nakahata.** 2003. Complete reconstitution of human lymphocytes from cord blood $CD34^+$ cells using the NOD/SCID/gammacnull mice model. Blood **102:**873–880.
12. **Ishihara, S., N. Tachibana, A. Okayama, K. Murai, K. Tsuda, and N. Mueller.** 1992. Successful graft of HTLV-I-transformed human T-cells (MT-2) in severe combined immunodeficiency mice treated with anti-asialo GM-1 antibody. Jpn. J. Cancer Res. **83:**320–323.
13. **Ishikawa, F., M. Yasukawa, B. Lyons, S. Yoshida, T. Miyamoto, G. Yoshimoto, T. Watanabe, K. Akashi, L. D. Shultz, and M. Harada.** 2005. Development of functional human blood and immune systems in NOD/SCID/IL2 receptor γ chain(null) mice. Blood **106:**1565–1573.
14. **Ito, M., H. Hiramatsu, K. Kobayashi, K. Suzue, M. Kawahata, K. Hioki, Y. Ueyama, Y. Koyanagi, K. Sugamura, K. Tsuji, T. Heike, and T. Nakahata.** 2002. NOD/SCID/gamma(c)(null) mouse: an excellent recipient mouse model for engraftment of human cells. Blood **100:**3175–3182.
15. **Legrand, N., T. Cupedo, A. U. van Lent, M. J. Ebeli, K. Weijer, T. Hanke, and H. Spits.** 2006. Transient accumulation of human mature thymocytes and regulatory T cells with CD28 superagonist in "human immune system" *Rag2*$^{-/-}\gamma_c^{-/-}$ mice. Blood **108:**238–245.
16. **Legrand, N., K. Weijer, and H. Spits.** 2006. Experimental models to study development and function of the human immune system in vivo. J. Immunol. **176:**2053–2058.
17. **Macchiarini, F., M. G. Manz, A. K. Palucka, and L. D. Shultz.** 2005. Humanized mice: are we there yet? J Exp. Med. **202:**1307–1311.
18. **Mazurier, F., A. Fontanellas, S. Salesse, L. Taine, S. Landriau, F. Moreau-Gaudry, J. Reiffers, B. Peault, J. P. Di Santo, and H. de Verneuil.** 1999. A novel immunodeficient mouse model—RAG2 x common cytokine receptor gamma chain double mutants—requiring exogenous cytokine administration for human hematopoietic stem cell engraftment. J. Interferon Cytokine Res. **19:**533–541.
19. **McCune, J., H. Kaneshima, J. Krowka, R. Namikawa, H. Outzen, B. Peault, L. Rabin, C. C. Shih, E. Yee, M. Lieberman, et al.** 1991. The SCID-hu mouse: a small animal model for HIV infection and pathogenesis. Annu. Rev. Immunol. **9:**399–429.
20. **Moffat, J. F., M. D. Stein, H. Kaneshima, and A. M. Arvin.** 1995. Tropism of varicella-zoster virus for human $CD4^+$ and $CD8^+$ T lymphocytes and epidermal cells in SCID-hu mice. J. Virol. **69:**5236–5242.
21. **Mosier, D. E., R. J. Gulizia, S. M. Baird, D. B. Wilson, D. H. Spector, and S. A. Spector.** 1991. Human immunodeficiency virus infection of human-PBL-SCID mice. Science **251:**791–794.
22. **Namikawa, R., H. Kaneshima, M. Lieberman, I. L. Weissman, and J. M. McCune.** 1988. Infection of the SCID-hu mouse by HIV-1. Science **242:**1684–1686.
23. **Poluektova, L. Y., D. H. Munn, Y. Persidsky, and H. E. Gendelman.** 2002. Generation of cytotoxic T cells against virus-infected human brain macrophages in a murine model of HIV-1 encephalitis. J. Immunol. **168:**3941–3949.
24. **Rozemuller, H., S. Knaan-Shanzer, A. Hagenbeek, L. van Bloois, G. Storm, and A. C. Martens.** 2004. Enhanced engraftment of human cells in RAG2/gammac double-knockout mice after treatment with CL2MDP liposomes. Exp. Hematol. **32:**1118–1125.
25. **Schauer, U., F. Stemberg, C. H. Rieger, W. Buttner, M. Borte, S. Schubert,**

H. Mollers, F. Riedel, U. Herz, H. Renz, and W. Herzog. 2003. Levels of antibodies specific to tetanus toxoid, *Haemophilus influenzae* type b, and pneumococcal capsular polysaccharide in healthy children and adults. Clin. Diagn. Lab Immunol. **10:**202–207.

26. **Shultz, L. D., B. L. Lyons, L. M. Burzenski, B. Gott, X. Chen, S. Chaleff, M. Kotb, S. D. Gillies, M. King, J. Mangada, D. L. Greiner, and R. Handgretinger.** 2005. Human lymphoid and myeloid cell development in NOD/LtSz-scid IL2R gamma null mice engrafted with mobilized human hemopoietic stem cells. J. Immunol. **174:**6477–6489.
27. **Traggiai, E., L. Chicha, L. Mazzucchelli, L. Bronz, J. C. Piffaretti, A. Lanzavecchia, and M. G. Manz.** 2004. Development of a human adaptive immune system in cord blood cell-transplanted mice. Science **304:**104–107.
28. **Trkola, A., H. Kuster, C. Leemann, A. Oxenius, C. Fagard, H. Furrer, M. Battegay, P. Vernazza, E. Bernasconi, R. Weber, B. Hirschel, S. Bonhoeffer, and H. F. Gunthard.** 2004. Humoral immunity to HIV-1: kinetics of antibody responses in chronic infection reflects capacity of immune system to improve viral set point. Blood **104:**1784–1792.
29. **van Maanen, M., and R. E. Sutton.** 2003. Rodent models for HIV-1 infection and disease. Curr. HIV Res. **1:**121–130.
30. **Watanabe, S., K. Terashima, S. Ohta, S. Horibata, M. Yajima, Y. Shiozawa, M. Z. Dewan, Z. Yu, M. Ito, T. Morio, N. Shimizu, M. Honda, and N. Yamamoto.** 15 September 2006. Hematopoietic stem cell-engrafted NOD/SCID/IL2Rγ null mice develop human lymphoid system and induce long-lasting HIV-1 infection with specific humoral immune responses. Blood doi:10.11.1182/blood-2006-04-017681. (Subsequently published, Blood **109:** 212–218, 2007.)
31. **Yahata, T., K. Ando, Y. Nakamura, Y. Ueyama, K. Shimamura, N. Tamaoki, S. Kato, and T. Hotta.** 2002. Functional human T lymphocyte development from cord blood $CD34^+$ cells in nonobese diabetic/Shi-scid, IL-2 receptor gamma null mice. J. Immunol. **169:**204–209.
32. **Yoder, M. C., J. G. Cumming, K. Hiatt, P. Mukherjee, and D. A. Williams.** 1996. A novel method of myeloablation to enhance engraftment of adult bone marrow cells in newborn mice. Biol. Blood Marrow Transplant. **2:**59–67.
33. **Zhang, H., F. Hoffmann, J. He, X. He, C. Kankasa, R. Ruprecht, J. T. West, G. Orti, and C. Wood.** 2005. Evolution of subtype C HIV-1 Env in a slowly progressing Zambian infant. Retrovirology **2:**67.